J Nanopart Res (2009) 11:333–340
DOI 10.1007/s11051-008-9385-0

RESEARCH PAPER

Gelatin–Chitosan composite capped gold nanoparticles: a matrix for the growth of hydroxyapatite

S. S. Liji Sobhana · J. Sundaraseelan · S. Sekar · T. P. Sastry · A. B. Mandal

Received: 20 December 2007 / Accepted: 20 March 2008 / Published online: 10 April 2008

Abstract Growth of hydroxyapatite (HA) on gelatin–chitosan composite capped gold nanoparticles is presented for the first time by employing wet precipitation methods and we obtained good yields of HA. Fourier transform infrared spectroscopy (FTIR) spectrum has shown the characteristic bands of phosphate groups in the HA. Scanning electron microscopy (SEM) pictures have shown spherical nanoparticles with the size in the range of 70–250 nm, whereas ≥2–50 nm sized particles were visualized in high resolution transmission electron microscopy (HR-TEM). X-ray diffraction (XRD) spectrum has shown Bragg reflections which are comparable with the HA. Energy dispersive X-ray (EDX) studies have confirmed calcium/phosphate stoichiometric ratio of HA. The thermogravimetric analysis (TGA) has shown about 74% of inorganic crystals in the nanocomposite formed. These results have revealed that gelatin–chitosan capped gold nanoparticles, acted as a matrix for the growth of HA.

S. S. L. Sobhana · J. Sundaraseelan · S. Sekar ·
T. P. Sastry (✉) · A. B. Mandal (✉)
Bio-products Lab, Central Leather Research Institute,
Adyar, Chennai 600020, India
e-mail: sastrytp@hotmail.com

A. B. Mandal
e-mail: clrim@vsnl.com

Keywords Gelatin–chitosan composite · Wet precipitation · Hydroxyapatite · Gold nanoparticles · Nanocomposite materials

Introduction

In the recent decades the death rate among the aged, due to bone defects which is the result of trauma, tumour ablation in orthopaedics or bone diseases is increasing and some of them die due to insufficient ideal bone substitute. Therefore some pioneering work should be done in the field of bone tissue engineering to prepare ideal bone substitute, which mimics the natural bone. The so-called work is a 'biomimetic approach' (Rose et al. 2002) and thus prepared bone substitute can help in the formation of osteogenic cells at the required site. Nanotechnology plays an important role in bone tissue engineering, as bone is a nanocomposite containing minerals and proteins essentially. The major portions of minerals in bone are apatites such as hydroxyapatite, fluoroapatite and carbonate apatite. From these apatites, hydroxyapatite is the commonly used bone mineral (Gineste et al. 1999), as it has osteoinductive nature (Liu et al. 1998). Hydroxyapatite can be used as a graft material for bone repair, augmentation, substitution (Chang et al. 2001). It is highly biocompatible, exhibits good bioactivity, osteoconductivity and it is resistant to injection (David et al. 2005) similar to that of a natural bone. The most important aspect of nHA is that it can promote the attachment and growth of human osteoblast-like cells (Huang et al. 2004). Gelatin has wide range of applications, one of which is that it can act as a protective medium in the synthesis of monodisperse colloidal particles in aqueous solution system (Borginon 1967). The attractive feature of gelatin is that it has not shown any antigenicity and is completely resorbable in vivo (Yao et al. 1996). Gelatin can be made into composites by blending with other materials like chitosan, β-tricalcium phosphate (β-TCP) and hydroxyapatite (HA). This composite has the property of imitating the natural extracellular matrix (ECM) for tissue engineering and cartilage with good results (Elcin et al. 1998).

Chitosan and its composites have been used in bone tissue engineering (Zhao et al. 2002). Chitosan (poly-1, 4, D-glucosamine) a partially de-acetylated derivative from chitin is structurally similar to glycosaminoglycan (GAG) and has many desirable properties as tissue engineering scaffolds (Suh et al. 2000). Chitosan finds extensive application due to its low cost, large-scale availability, antimicrobial activity (Khor and Lim 2003), biodegradability, non-toxicity and its adsorption properties (Dufresne et al. 1999). The free amino group in chitosan has chelating, film forming properties and is soluble 0.3 N acetic acid. The mechanical and the biological properties of chitosan can be increased by blending it with gelatin which has the capacity to form polyelectrolyte complex (Mao et al. 2003) and has found much attention in bone replacements. The gelatin–chitosan network has been found to be safe, haemostatic and osteoinductive and does a good work on wound healing (Rezania and Healy 1999).

In a 3D porous hydroxyapatite/chitosan–gelatin [HCG] scaffold, Zhao et al. (2006) found that human mesenchymal stem cells [HMS] are maintained at a high proliferation rate. Du et al. (1999) used a biomimetic nano-HA/collagen scaffold with osteogenic cells in organ culture. Natural biopolymers such as collagen, fibrin, alginate and hyaluronic acid (Geiger et al. 2003), can be used in bone tissue engineering. Synthetic polymers such as poly (α-hydroxyl acids), poly (lactic acid) PLA (Mikos et al. 1994), poly (glycolic acid) PGA (Ma et al. 1995) or their co-polymer PLGA (Shea et al. 2000) can also be used as biomaterials for the use in bone tissue engineering.

The development of metal nanoparticles with well-defined shape, size and composition is a big challenge in the field of nanotechnology. Several methods have been reported for the preparation of metal nanoparticles (Kometani et al. 2001) to control the size (Murphy et al. 2005) and shape (Sun et al. 2002) of nanoparticles. Gold nanoparticles (AuNPs) can be synthesized by the reduction of Chloroauric acid ($HAuCl_4$) using citrate (Su et al. 2003; Misra et al. 2006), sodium borohydride ($NaBH_4$) as reducing agents to synthesize AuNPs in organic solvents (Manna et al. 2003). AuNPs can also be prepared by reducing with chitosan, in which chitosan acts as a stabilizing agent and a protecting polymer (Esumi et al. 2003). But chitosan is having poor solubility in neutral and basic medium; therefore, it is necessary to provide an acidic medium like hydrochloric acid, lactic acid, acetic acid, glutamic acid to dissolve chitosan. Esumi et al. (2003) reported the formation of gold–chitosan nanocomposite by adsorption of chitosan molecules on particle surfaces and evaluated the catalytic activities from elimination of hydroxyl radicals using a spin-trapping technique.

Aryal et al. (2006) have shown that gold nanoparticles with collagen form an efficient matrix for the growth of HA and the mineralized collagen can be potentially applied in bone tissue repair and regeneration. He has also demonstrated the immobilization of fibrous collagen onto gold nanoparticles thereby engineering the fibres into nanospheres which were subsequently used for the synthesis of HA. In the present study, the preparation of hydroxyapatite nanoparticles on gelatin–chitosan capped gold nanoparticles is discussed. The novelty of this study lies in the usage of chitosan along with gelatin and the yield of nano-HA is about 74%.

Experimental details

Reagents

Sodium borohydride, Hydrogen tetrachloroaurate (III), 30 wt.% solution in dilute hydrochloric acid, 99.99% was purchased from Sigma-Aldrich St. Louis, MO, USA. Sodium dihydrogen ortho-Phosphate was purchased from Qualigens Fine chemicals, India. Calcium chloride dihydrate extra pure was purchased from Merck Ltd., India. Gelatin of pharmaceutical grade was used and other chemicals used were of analytical grade. Chitosan was prepared by the modification of earlier methods (Mochizuki et al. 1989).

Nanoparticle synthesis

One gram of gelatin (G) was dissolved in 50 mL of double distilled water at 55 °C. One gram of Chitosan (C) was dissolved in 50 mL of 0.1 N HCl. To 1 mL of gelatin solution, 1 mL of chitosan solution was added and stirred at room temperature till the solution mixture was homogenous (GC). As gelatin is soluble in water and could not be precipitated because of its ambiguous isoelectric point chitosan solution was added to the gelatin solution (chitosan can be precipitated above pH 6.5 along with gelatin). To 2 mL of GC solution, 0.5 mL of aqueous $HAuCl_4$ solution (0.01 M) was added followed by stirring for 1 h. At this time the pH of the solution was around 6. To this resulting solution 0.2 mL of 1 M $NaBH_4$ dissolved in 0.3 M NaOH solution was added dropwise followed by stirring for 1 h. The solution developed a wine red colour. Later the pH of the solution was brought to 7 using dilute HCl (0.1 N). A fair pink colour was observed which is the characteristic colour of gold nanoparticles. The contents were centrifuged at 6,000 rpm for 15 min; the pellet formed was purified by repeatedly washing with double distilled water to ensure that it was free from any impurities for the preparation of hydroxyapatite. The pellet (GC–Au nanomatrix) was dispersed in 5 mL double distilled water and to this solution 1 mL of $CaCl_2$ solution (1 M) was added followed by addition of 1 mL of $NaH_2PO_4 \cdot 12H_2O$ solution (1 M), and the contents were stirred for half an hour at room temperature (30 °C). The resulting precipitate was centrifuged and washed repeatedly with water. Finally the HAP formed was dried at100 °C for about 5 h. The mechanism of the formation of HAP is schematically shown in Fig. 1.

A separate control experiment was conducted as above except that $HAuCl_4$ solution and $NaBH_4$ solution were not added in the reaction mixture.

Characterization

FTIR for the GC–Au–HAp nanocomposite was carried out using Nicolet impact 400 Fourier Transform Infrared Spectroscopy (FTIR). Surface structure was visualized by scanning electron microscope (SEM, JEOL JSM-5610LB) with Phoenix EDX attachment, which was directly connected to SEM to carry out the elemental analysis of the same. Dried and powdered samples were coated with gold ions using an ion coater (Fisons sputter coater) under the following conditions: 0.1 Torr pressure, 20 mA current and 70 s coating time, using a 15 KV accelerating voltage. The EDX spectrum was recorded in a spot-profile mode by focusing the electron beam onto the specific regions of the sample. Thermo gravimetric analysis (TGA) was carried out using TGA Q50 V20.6 thermal analyser Build 31 in

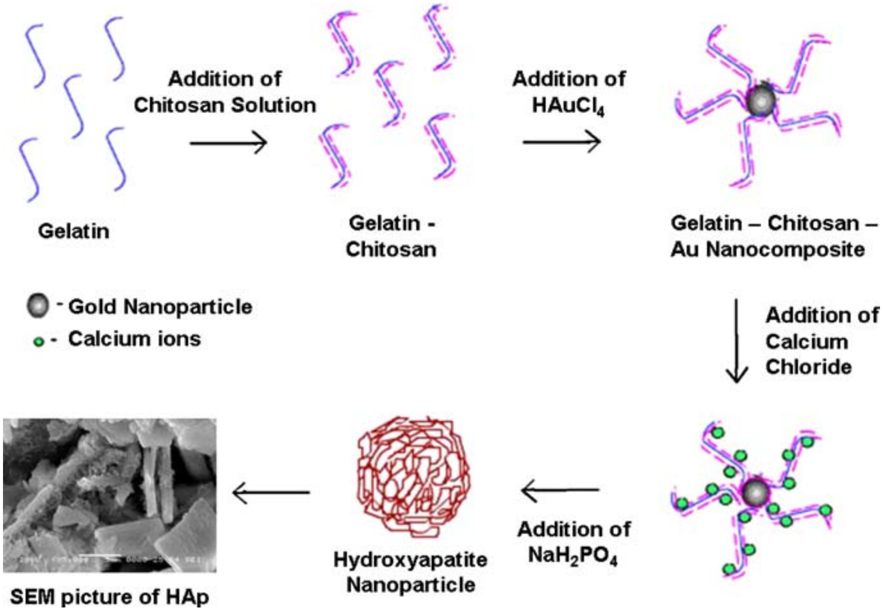

Fig. 1 Schematic representation of mechanism of formation of GC–Au–HA nanocomposite

nitrogen atmosphere (80 mL/min) at a heating rate of 10 °C/min. The particle size and morphology of the samples were studied using High Resolution-Transmission Electron Microscope (HR-TEM) using JEM-3010F transmission electron microscopy (TEM). A drop of well-dispersed nanoparticle dispersion was placed onto the amorphous carbon–coated 200-mesh copper grid, followed by drying the sample at ambient temperature before it was loaded into the microscope. X- ray diffraction (XRD) pattern was recorded from a drop-coated sample on a glass substrate.

Results and discussion

As gelatin is soluble in water with ambiguous isoelectric point we have prepared gelatin–chitosan composite that precipitates at pH around 7. As the backbone of gelatin molecule contains carboxylic groups, the calcium ions of the calcium chloride bind to these groups and further calcium ions react with phosphate ions (from NaH_2PO_4) to form a compound like HAP. Addition of chitosan solution to gelatin solution is first reported in this article to prepare gold-based HAP nanoparticles.

Figure 2a shows the X-ray diffraction (XRD) pattern of HAP crystals using gelatin–chitosan capped gold nanoparticles as a scaffold. The XRD pattern was recorded from a drop-coated sample of HAP on a glass substrate. The peaks at 31.7, 45.3 and 56.2 indicate reflections from 112, 222, 004 crystal planes, respectively. These reflections more or less correspond to Bragg reflections of HAP. The result shows that gold nanoparticles induced the formation of HAP nanoparticles on the gelatin–chitosan scaffold. Figure 2b shows the XRD spectrum of the precipitate formed in the control experiment showing peaks other than HA. These peaks include α-TCP with peaks at 21.6, 23.4 and 25.5, and β-TCP with peaks at 27.3 and 28.4 (Park et al. 2008). Without gold nanoparticles it is clear from this results that in the absence of gold nanoparticles, other calcium apatites will form when gelatin and Chitosan are used as a medium.

The surface morphology of the GC–Au capped nanoparticles analysed by scanning electron microscope (SEM) is shown in Fig. 3a, b, c. In Fig. 3a, the size and shape of the individual crystals can be observed. The shape of the crystals is spherical and the sizes of the crystals are in the range of 70 to 250 nm. A beautiful aggregation of these crystals is shown in Fig. 3b, c. The aggregated HA particles exhibited crystalline nature. The High-resolution transmission electron microscopic (HR-TEM) analysis in Fig. 4b has revealed that the size of the nanocomposite formed was in the range of ≥2–50 nm. The aggregations of these nanoparticles are represented in Fig. 4a. The selected area of diffraction in Fig. 4c of the HA shows the Bragg deflections at 004, 112, 222. These studies have confirmed the nanosized components of GC–Au–HA nanocomposite.

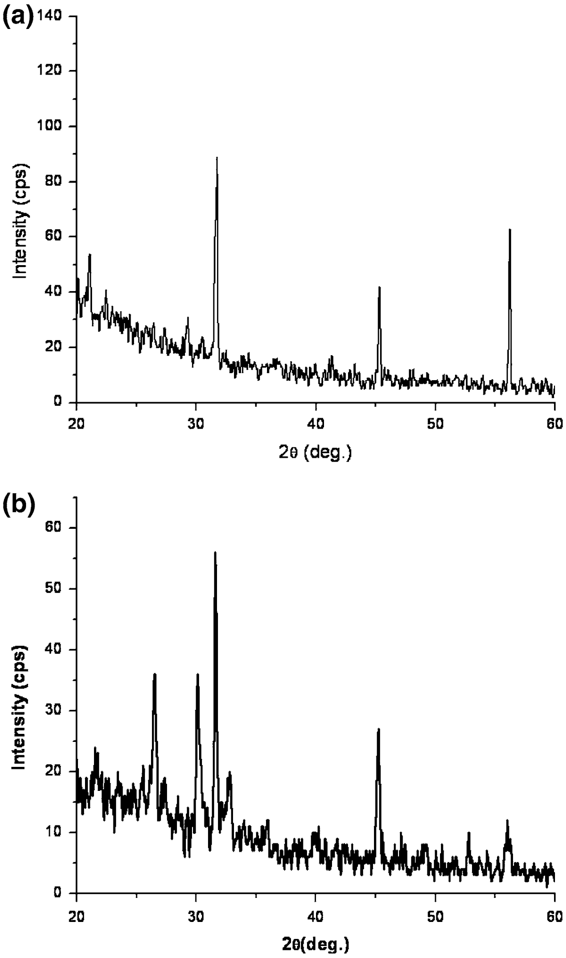

Fig. 2 (**a**) XRD pattern of GC–Au–HA nanocomposite exhibiting the peaks at 31.7, 45.3 and 56.2. (**b**) XRD spectrum of the precipitate obtained in control experiment exhibiting peaks of α-TCP with peaks at 21.6, 23.4 and 25.5 and β-TCP with peaks at 27.3 and 28.4 apart from HA peaks

The Energy dispersive spectroscopy (EDX) spectrum of the nanocomposite formed is shown in

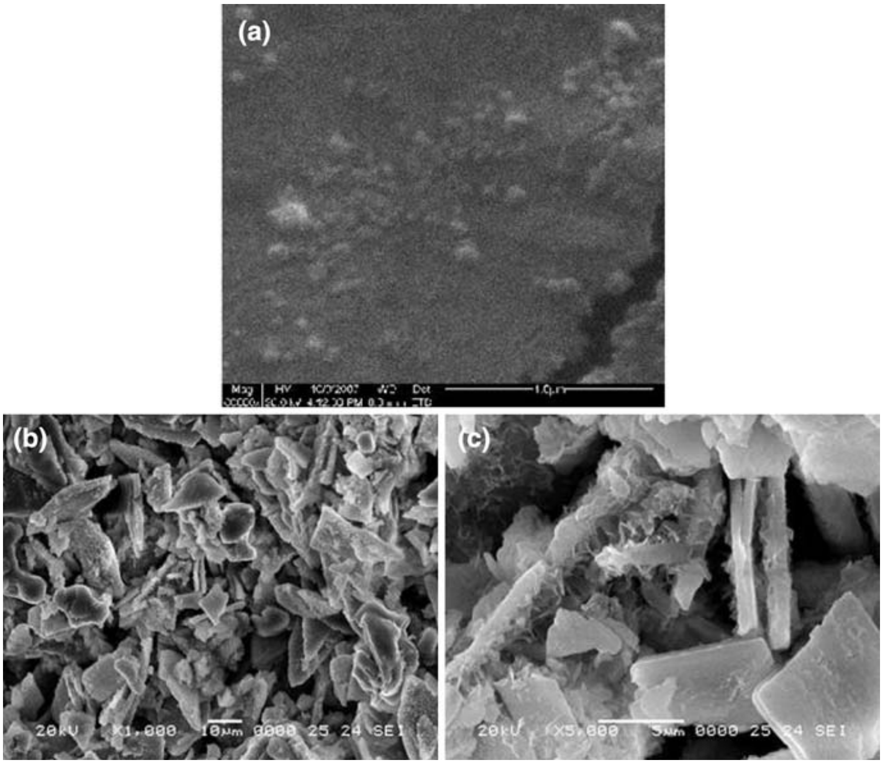

Fig. 3 Scanning Electron Microscope image of the GC–Au–HA nanocomposite (**a**) showing individual crystals with the size in the range 70 to 250 nm (**b**) and (**c**) showing aggregated crystals

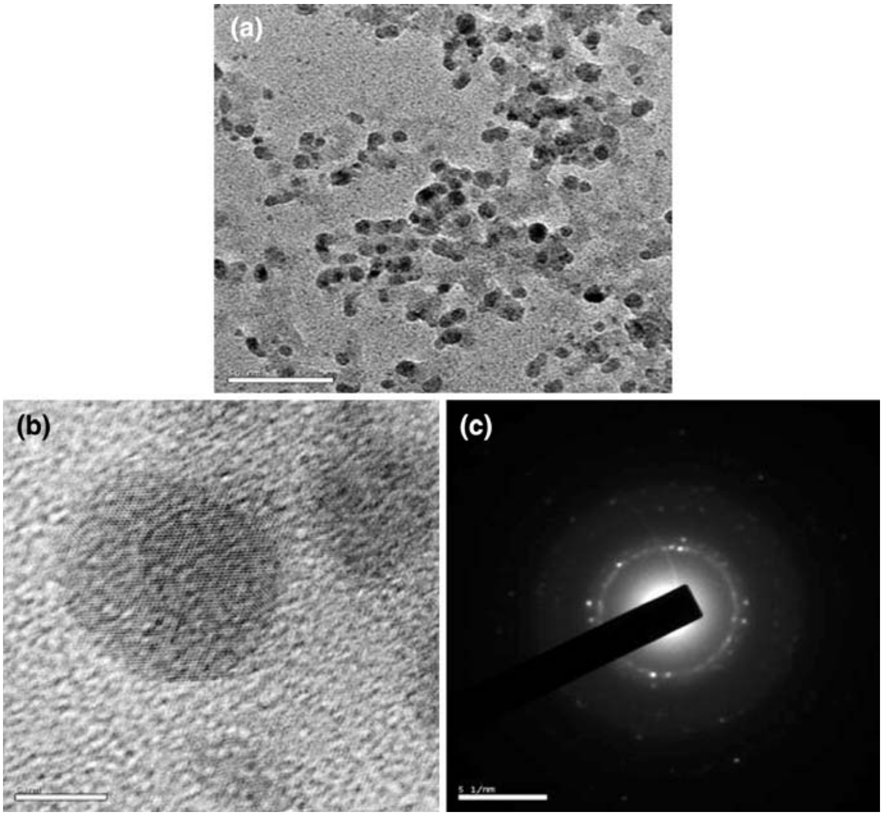

Fig. 4 High Resolution Transmission Electron Microscope images of GC–Au–HA nanocomposite showing the size of nanocomposite (**a**) 50 nm (**b**) 5 nm (**c**) diffraction image of the composite showing the lattice parameters at 004, 112, 222

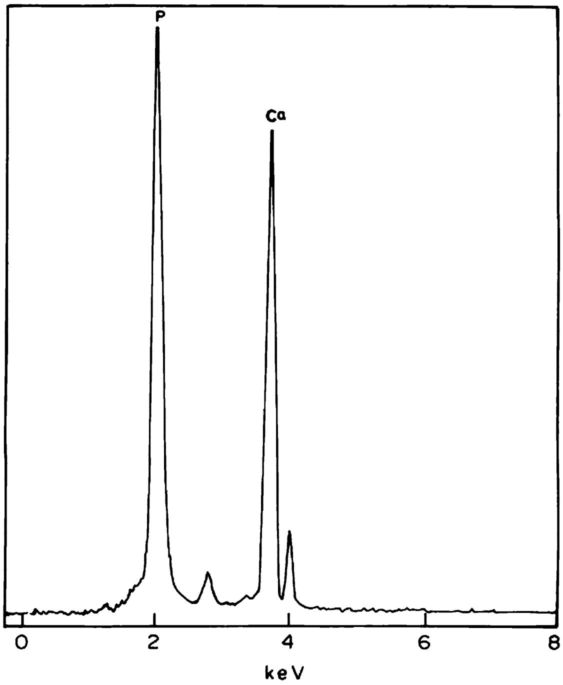

Fig. 5 EDX profile showing the Ca and P signals of GC–Au–HA nanocomposite

Fig. 5. The calcium and phosphorus signals are very clearly seen indicating the formation of calcium phosphates. The ratio of Ca to P was found to be 1.64:1 and the value is similar with that of synthetic HA.

The Fourier transform infrared spectroscopy (FTIR) spectrum of the HA formed using GC–Au–HA nanoparticles is seen in Fig. 6a. The vibration modes υ_1, υ_3, υ_4 of the phosphate ions are observed in the spectrum. υ_3 band was observed around 1,063 cm^{-1} and well-resolved bands at 602, 576 and 658 represent υ_4 vibration modes. The peak at 873 shows the contribution of HPO_4^{-3} ions, a weak υ_1 vibration mode of the phosphate groups is seen at 986 cm^{-1}. The FTIR spectrum of the precipitate formed in the control experiment is shown in Fig. 6b. It did not differ much with that of HA formed using gold nanoparticles and exhibits similar phosphate vibrations.

The thermogram of GC–Au–HA nanocomposite is shown in Fig. 7a. The composite loses its moisture and the bound water up to 199 °C. Approximately 5% protein loss was observed between 199 and 429 °C which is due to the degradation of gelatin. Around 11% loss was observed between 429 and 825 °C which was attributed to further degradation of the material or evolution of CO_2. The remaining 74% of the inorganic material is considered as HA, whereas the thermogram of the precipitate obtained in the control experiment (Fig. 7b) shows 62% of the inorganic material at 785 °C. About 12% more inorganic material formed in the experiment using gold nanoparticles indicates a better yield.

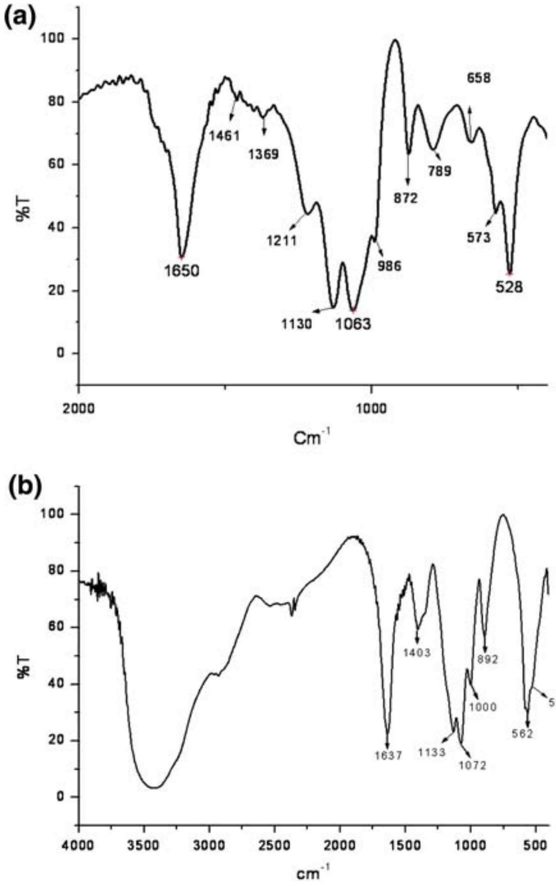

Fig. 6 (**a**) FTIR of the GC–Au–HA nanocomposite showing the phosphate vibrational modes of v_1, v_2, v_4 of HA. (**b**) FTIR of the precipitate obtained in control experiment

Conclusions

It is evident from the study that gelatin–chitosan capped gold nanoparticles can act as a matrix for the growth of HAp crystals. We were able to produce HAp nanoparticles on the surface of gelatin–chitosan

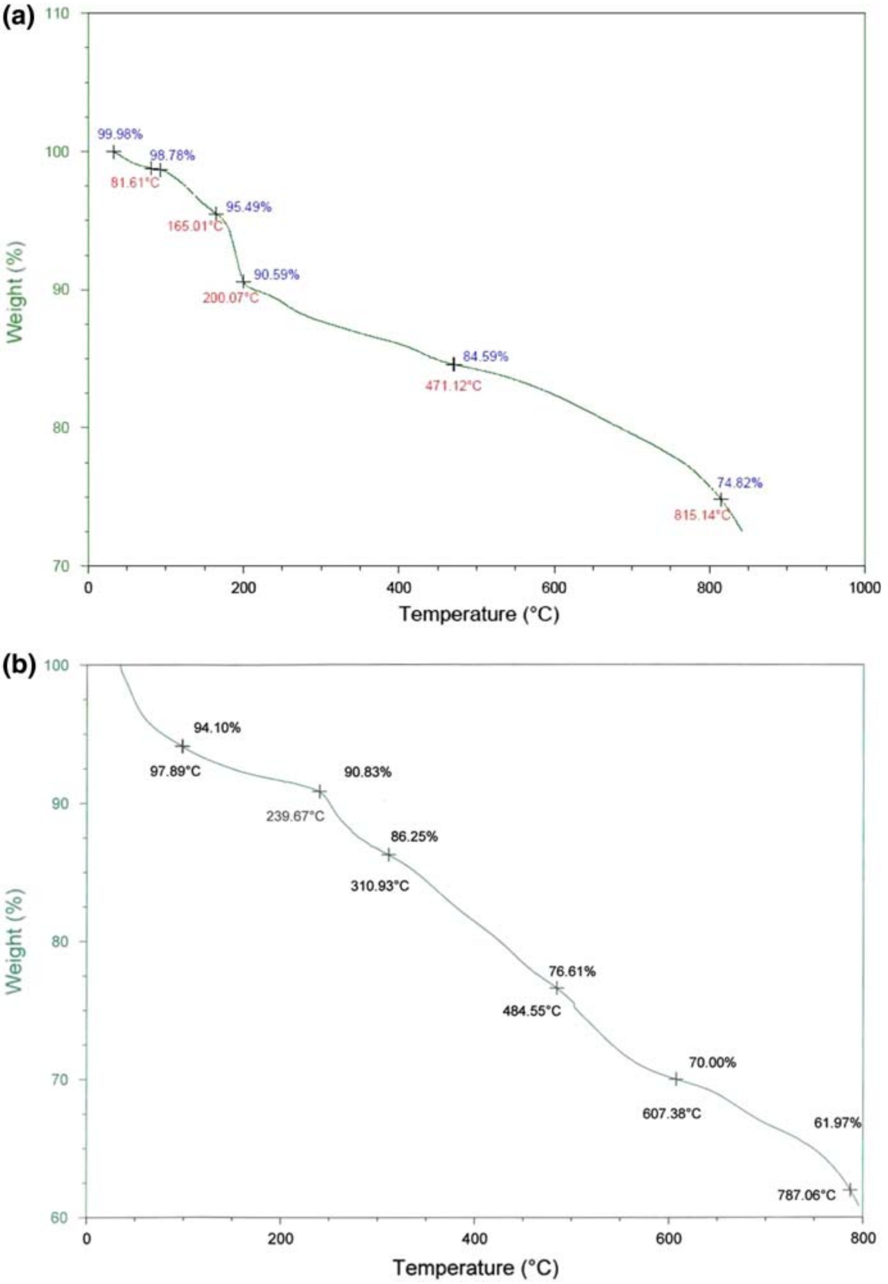

Fig. 7 (**a**) Thermogram of the GC–Au–HA nanocomposite exhibiting the two stage weight loss due to the decomposition of gelatin and Chitosan. (**b**) Thermogram of the precipitate obtained in control experiment

capped gold nanoparticles in this study. This method is cost-effective with a yield of 74% nano-HA.

References

Aryal S, Bahadur R, Bhattarai SR, Prabu P, Kim HY (2006) Immobilization of collagen on gold nanoparticles: preparation, characterization, and hydroxyapatite growth. J Mater Chem 16:4642–4648

Borginon H (1967) Photographic properties of the gelatin macromolecule. J Photogr Sci 15:207–214

Chang MC, Ikoma T, Kikuchi M, Tanaka J (2001) Preparation of a porous hydroxyapatite/collagen nanocomposite using glutaraldehyde as a crosslinkage agent. J Mater Sci Lett 20:1199–1201

David L, Argenta L, Fisher D (2005) Hydroxyapatite cement in pediatric craniofacial reconstruction. J Craniofac Surg 16:129–133

Du C, Cui FZ, Zhu XD, de Groot K (1999) Three-dimensional nano-HAp/collagen matrix loading with osteogenic cells in organ culture. J Biomed Mater Res 44:407–415

Dufresne A, Cavaille JY, Dupeyre D, Garcia-Ramirez M, Romero J (1999) Morphology, phase continuity and mechanical behaviour of polyamide 6 chitosan blends. Polymer 40:1657–1666

Elcin AE, Elcin YM, Pappas GD (1998) Neural tissue engineering: adrenal chromaffin cell attachment and viability on chitosan scaffolds. Neurol Res 20:648–654

Esumi K, Takei N, Yoshimura T (2003) Antioxidant-potentiality of gold–chitosan nanocomposites. Colloids Surf B Biointerfaces 32:117–123

Geiger M, Li RH, Friess W (2003) Collagen sponges for bone regeneration with rhBMP-2. Adv Drug Deliv Rev 55:1613–1629

Gineste L, Gineste M, Ranz X, Ellefterion A, Guilhem A, Rouquet N, Frayssinet P (1999) Degradation of hydroxylapatite, fluorapatite, and fluorhydroxyapatite coatings of dental implants in dogs. J Biomed Mater Res 48:224–234

Huang J, Best SM, Bonfield W, Brooks RA, Rushton N, Jayasinghe SN, Edirisinghe MJ (2004) In vitro assessment of the biological response to nano-sized hydroxyapatite. J Mater Sci Mater Med 15:441–445

Khor E, Lim LY (2003) Implantable applications of chitin and chitosan. Biomaterials 24:2339–2349

Kometani N, Tsubonishi M, Fujita T, Asami K, Yonezawa Y (2001) Preparation and optical absorption spectra of dye-coated Au, Ag, and Au/Ag colloidal nanoparticles in aqueous solutions and in alternate assemblies. Langmuir 17:578–580

Liu Q, de Wijn JR, van Blitterswijk CA (1998) A study on the grafting reaction of isocyanates with hydroxyapatite particles. J Biomed Mater Res 40:358–364

Ma PX, Langer R (1995) In: Mikos AG et al (eds) Polymers in medicine and pharmacy. MRS, Pittsburgh, pp 99–104

Manna A, Chen PL, Akiyama H, Wei TX, Tamada K, Knoll W (2003) Optimized photoisomerization on gold nanoparticles capped by unsymmetrical azobenzene disulfides. Chem Mater 15:20–28

Mao JS, Zhao LG, Yin YJ, Yao KD (2003) Structure and properties of bilayer chitosan–gelatin scaffolds. Biomaterials 24:1067–1074

Mikos AG, Thorsen AJ, Czerwonka LA, Bao Y, Langer R, Winslow DN, Vacanti JP (1994) Preparation and characterization of poly(L-lactic acid) foams. Polymer 35:1068–1077

Misra TK, Chen TS, Liu CY (2006) Phase transfer of gold nanoparticles from aqueous to organic solution containing resorcinarene. J Colloid Interface Sci 297:584–588

Mochizuki A, Sato Y, Ogawara H, Yamashita S (1989) Pervaporation separation of water/ethanol mixtures through polysaccharide membranes. II. The permselectivity of chitosan membrane. J Appl Polym Sci 37(12):3375–3384

Murphy CJ, San TK, Gole AM, Orendorff CJ, Gao JX, Gou L, Hunyadi SE, Li T (2005) Anisotropic metal nanoparticles: synthesis, assembly, and optical applications. J Phys Chem B 109:13857–13870

Park YM, Ryu SC, Yoon SY, Stevens R, Park HC (2008) Preparation of whisker-shaped hydroxyapatite/β-tricalcium phosphate composite. Mater Chem Phys, doi: 10.1016/j.matchemphys.2007.12.013

Rezania A., Healy KE (1999) Biomimetic peptide surfaces that regulate adhesion, spreading, cytoskeletal organization, and mineralization of the matrix deposited by osteoblast-like cells. Biotechnol Prog 15:19–32

Rose F., Oreffo ROC, Nf (2002) Bone tissue engineering: hope vs hype. Biochem Biophys Res Commun 292:1–7

Shea LD, Wang D, Franceschi RT, Mooney DJ (2000) Engineered bone development from a pre-osteoblast cell line on three-dimensional scaffolds. Tissue Eng 6:605–617

Su CH, Wu PL, Yeh CS (2003) Sonochemical synthesis of well-dispersed gold nanoparticles at the ice temperature. J Phys Chem B 107:14240–14243

Suh JKF, Matthew HWT (2000) Application of chitosan-based polysaccharide biomaterials in cartilage tissue engineering: a review. Biomaterials 21:2589–2598

Sun YG, Xia YN (2002) Shape-controlled synthesis of gold and silver nanoparticles. Science 298:2176–2179

Yao CH, Sun JS, Lin FH, Liao CJ, Huang CW (1996) Biological effects and cytotoxicity of tricalcium phosphate and formaldehyde cross-linked gelatin composite. Mater Chem Phys 45:6–14

Zhao F, Grayson WL, Ma T, Bunnell B, Lu WW (2006) Effects of hydroxyapatite in 3-D chitosan–gelatin polymer network on human mesenchymal stem cell construct development. Biomaterials 27:1859–1867

Zhao F, Yin YJ, Lu WW, Leong JC, Zhang WJ, Zhang JY, Zhang MF, Yao KD (2002) Preparation and histological evaluation of biomimetic three-dimensional hydroxyapatite/chitosan–gelatin network composite scaffolds. Biomaterials 23:3227–3234